Improved laser-beam uniformity using the angular dispersion of frequency-modulated light

S. Skupsky, R. W. Short, T. Kessler, R. S. Craxton, S. Letzring, and J. M. Soures
Laboratory for Laser Energetics, University of Rochester, 250 East River Road, Rochester, New York 14623-1299

(Received 24 March 1989; accepted for publication 12 June 1989)

A new technique is presented for obtaining highly smooth focused laser beams. This approach is consistent with the constraints on frequency tripling the light, and it will not produce any significant high-intensity spikes within the laser chain, making the technique attractive for the high-power glass lasers used in current fusion experiments. Smoothing is obtained by imposing a frequency-modulated bandwidth on the laser beam using an electro-optic crystal. A pair of gratings is used to disperse the frequencies across the beam, without distorting the temporal pulse shape. The beam is broken up into beamlets, using a phase plate, such that the beamlet diffraction-limited focal spot is the size of the target. The time-averaged interference between beamlets is greatly reduced because of the frequency differences between the beamlets, and the result is a relatively smooth diffraction-limited intensity pattern on target.

I. INTRODUCTION

A new technique is being examined to improve the quality of focused, high-power laser beams beyond the level that has already been achieved with the distributed phase plates (DPPs) currently used in laser-fusion experiments.[1] These phase plates break each beam into beamlets whose diffraction-limited focal spot equals the size of the irradiated target.[2] However, superimposed on the smooth diffraction-limited intensity envelope is a rapidly varying intensity structure arising from the interference between the different beamlets (Fig. 1). Once a plasma atmosphere has formed around the target, much of the short-wavelength structure in the laser-energy deposition is expected to be smoothed by thermal conduction within the target as heat is transported from the place of energy deposition to the ablation surface. However, before thermal smoothing becomes effective, this structure could imprint itself on the target surface and "seed" the Rayleigh–Taylor instability, much like a target surface imperfection. The longer-wavelength interference structure might never be adequately smoothed and could drive a distorted implosion. The goal of the work described here is to develop a technique to reduce the effect of the interference structure, while retaining the smooth intensity envelope.

The strategy employed is to vary the interference pattern on a time scale Δt that is short compared to the characteristic hydrodynamic response time of the target. At any instant of time, a highly modulated intensity pattern will be present, but the intensity averaged over Δt will be smooth. The interference pattern can be varied by rapidly shifting the beam, or rapidly changing the relative phases between the individual beamlets. An example of the latter approach is induced spatial incoherence (ISI).[3] But ISI might not be a good candidate for a frequency-tripled glass-laser system such as OMEGA at the University of Rochester, since the required "chaotic" broad bandwidth light could be difficult to frequency-triple efficiently, and, unless the bandwidth is phase modulated, it would produce high-intensity temporal spikes within the laser that could damage the laser glass. Therefore, we have been considering an alternate scheme, smoothing by spectral dispersion (SSD) of the laser light. SSD combines aspects of both shifting the beam and changing the phase. Like ISI, it requires a bandwidth, but the smoothing mechanism is different, permitting the use of a nonchaotic bandwidth and allowing high-efficiency frequency tripling. The general concept of SSD is to spectrally disperse broad-bandwidth light onto a phase plate so that, ideally, each element of the DDP is irradiated by a different frequency.[4] The relative phase between beamlets from different phase-plate elements will then vary in time according to their frequency differences. The larger the bandwidth, the more rapidly the structure will change and the more rapidly the time-averaged intensity will smooth. However, if some phase-plate elements have the same "color" (frequency), a residual interference structure will be produced that will not smooth.

As an example, consider the interference between the two rays shown in Fig. 1. In the target plane their combined electric fields are

$$E = E_1 e^{i(kL_1 + \phi_1 - \omega t)} + E_2 e^{i(kL_2 + \phi_2 - \omega t)},$$

where the amplitudes are of the diffraction limited form $E_1 \sim E_2 \sim \sin(y)/y$, and ϕ_1 and ϕ_2 are the phases of the rays (including those imposed by the phase plate). For simplicity, take $E_1 = E_2$. Then the intensity variation is

$$I = |E|^2 = 2E_1^2 + 2E_2^2 \cos[k(L_1 - L_2) + (\phi_1 - \phi_2)],$$

which results in high-intensity fluctuations in the transverse (y) direction as the pathlength difference $(L_1 - L_2)$ changes. Now, letting the rays have different frequencies and wave numbers, (ω_1, k_1) and (ω_2, k_2), the intensity becomes

$$I = 2E_1^2 + 2E_1^2 \cos[k_1L_1 - k_2L_2 + (\phi_1 - \phi_2) + (\omega_1 - \omega_2)t].$$

At any instant of time, the intensity pattern will still have high-intensity modulations, but they will fluctuate in time according to the frequency difference. When averaged over

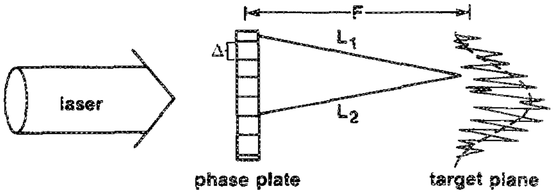

FIG. 1. The phase-plate intensity pattern in the focal plane consists of a diffraction-limited envelope upon which is superimposed a rapidly varying structure caused by the interference between rays from different phase-plate elements.

time, the interference term will approach zero as $1/(\omega_1 - \omega_2)t$, and the intensity will approach the smooth diffraction-limited sinc^2 envelope.

One constraint on the development of SSD has been that it must accommodate high-efficiency frequency tripling of the broad-bandwidth light. [Current laser fusion experiments use frequency-tripled infrared (IR) light to take advantage of the increased collisional laser absorption and higher hydrodynamic implosion efficiency that is possible at shorter wavelengths.] High-efficiency tripling can be achieved only over a narrow spread in wavelengths (~ 1 Å in the IR) for a given orientation of the tripling crystals. The strategy is to impose slightly different directions of propagation on the different frequencies in the bandwidth so that each frequency will be incident on the tripling crystals at the optimal angle for that wavelength. This can be accomplished in two ways: If the light can be spectrally dispersed so that the wavelength is linearly increasing in one direction, then cylindrical lenses can be used to impose the required angular spread.[4] If it is not practical to attain the linear wavelength dispersion, then the required angular spread can be imposed by a diffraction grating. The latter approach is used here. A method for implementing a limited version of SSD on the OMEGA laser system is described below. This relatively simple technique will not eliminate all the interference structure, but it takes a major step in that direction without significantly degrading the performance of the high-power frequency-tripled laser system. Further improvements in uniformity are possible with other variations of SSD that are presently under investigation.

II. IMPLEMENTATION CONSIDERATIONS FOR SSD

To implement SSD on a laser system such as OMEGA, a number of key requirements must be met: (1) generation of bandwidth that will not damage the laser glass with high-intensity spikes; (2) dispersion of the bandwidth frequencies across the DPP elements; (3) high-efficiency frequency tripling; (4) identification of a dispersing configuration that will not significantly distort the temporal profile of the beam; and (5) obtaining the improved uniformity over a sufficiently small averaging time.

A. Bandwidth source

One form of bandwidth that can be easily propagated through a glass laser system is that generated by phase modulation of the beam. The phase-modulated electric field is of the form[5] $E(t) = E_0(t)e^{i\Phi(t)}$, where the entire effect of bandwidth on the original field E_0 is contained in the time-varying phase. [The bandwidth associated with the time variation of $E_0(t)$ is negligible for typical nanosecond pulses.] The laser intensity varies as $|E(t)|^2 = |E_0(t)|^2$ and contains no additional high-intensity spikes from the interference between different frequencies. This would not be true for the "chaotic" form of bandwidth in which the different modes have random phases [i.e., $E(t) = \Sigma\, a_n\, e^{i(\omega_n t + \phi_n)}$ where ϕ_n is random].

One relatively simple form of phase modulation can be obtained by passing the laser beam through an electro-optic (EO) crystal with an imposed oscillating electric field. The effect is to produce a laser electric field of the form:

$$E(t) = E_0\, e^{i\omega t + i\delta \sin \omega_m t}, \tag{1}$$

where δ and ω_m are the modulation amplitude and angular frequency of the E-O device, and ω is the fundamental angular frequency of the laser. By expanding the exponential term in a Fourier series[5]:

$$E(t) = E_0 \sum_{-\infty}^{\infty} J_n(\delta) e^{i(\omega + n\omega_m)t}, \tag{2}$$

we see that the beam contains frequency side bands in increments of ω_m, which extend out to approximately $\pm\,\delta\omega_m$, at which point the mode amplitudes (J_n) rapidly approach zero; i.e., the frequency spread is well approximated by $\Delta\nu = 2\delta\nu_m$, in terms of the modulation amplitude and frequency.

B. Bandwidth dispersion

A crucial element of SSD is that a large number of DPP elements must be irradiated by different frequencies at each instant of time. The EO phase-modulated beam, by itself, would not be adequate for SSD, because at any time all DPP elements would be irradiated by only a single dominant frequency given by the time derivative of the phase in Eq. (1). We now show that adding angular dispersion to the phase-modulated beam by means of a diffraction grating will result in the desired variation of frequency across the beam (as well as enhance frequency conversion). If we model the light emerging from the grating as plane waves with the amplitude of each frequency component given by Eq. (2), then the spectrally dispersed beam is described by

$$E_D = E_0 \sum_n J_n(\delta) e^{i(\omega + n\omega_m)t - i\mathbf{k}_n\cdot\mathbf{R}}, \tag{3}$$

where

$$\mathbf{k}_n\cdot\mathbf{R} = (1/c)(\omega + n\omega_m)[Z\cos\theta_n + Y\sin\theta_n].$$

The Z axis is chosen along the propagation direction of the fundamental frequency ($n = 0$), and the dispersion angle for the nth harmonic, θ_n, is given in terms of the grating dispersion $\Delta\theta/\Delta\lambda$:

$$\theta_n = \frac{d\theta}{d\omega} n\omega_m = -\frac{\Delta\theta}{\Delta\lambda}\frac{\lambda}{\omega} n\omega_m.$$

Keeping terms linear in the small quantity ω_m/ω, Eq. (3)

becomes

$$E_D(Z,Y,t) \approx E_0\, e^{i\omega t - ikZ} \sum_n J_n(\delta)$$
$$\times \exp\left[in\omega_m \left(t - \frac{Z}{c} + \frac{\Delta\theta}{\Delta\lambda}\frac{\lambda}{c} Y \right)\right], \qquad (4)$$

which can be recombined as

$$E_D = E_0\, e^{i\omega t - ikZ + i\delta \sin[\omega_m(t - Z/c) + \alpha Y]}, \qquad (5)$$

where

$$\alpha = 2\pi \frac{\Delta\theta}{\Delta\lambda}\frac{\omega_m}{\omega}.$$

To this approximation, we see that the beam is still purely phase modulated after dispersion (though the terms of higher order in ω_m/ω can produce amplitude modulation if the beam propagates far enough, typically tens of meters). In fact, any dispersive mechanism for which the phase varies linearly with wavelength will leave the beam phase modulated.

The instantaneous frequency now varies across the beam with a wavelength of $2\pi/\alpha$. If this is smaller than the beam diameter, then the full range of the modulated spectrum will be present simultaneously across the phase plate, with different areas of the DPP illuminated by different frequencies. Although the instantaneous frequency only varies in one direction, it will be seen to produce a substantial improvement in uniformity.

The "color" variation across the beam can be viewed as the result of a spatially varying time delay across the beam. From Eq. (5), the total time delay is proportional to the grating dispersion and beam diameter:

$$t_D = \left(D \frac{\Delta\theta}{\Delta\lambda} \right) \frac{\lambda}{c}. \qquad (6)$$

(The quantity in parentheses is constant throughout the laser system because the beam divergence changes inversely with the diameter.) Unfortunately, a straightforward extension of this analysis shows that the finite pulse envelope of the beam, also acquires a y-dependent time delay, i.e., the amplitude function $E_0(t)$ becomes $E_0(t - \alpha Y)$ after dispersion, as shown in Fig. 2. Not only is the pulse lengthened, but there is an intensity variation across the beam aperture. This

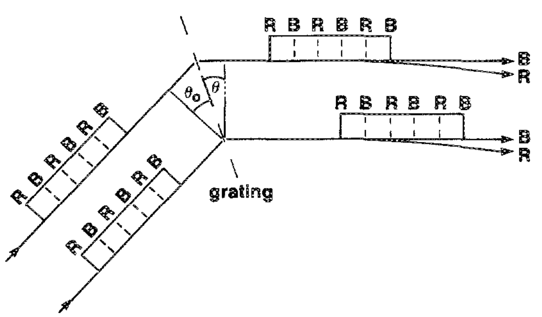

FIG. 2. The diffraction grating introduces a time delay across the beam in addition to angular dispersion of the spectrum. The "R" and "B" labels represent the places where the "red" and "blue" ends of the spectrum are dominant.

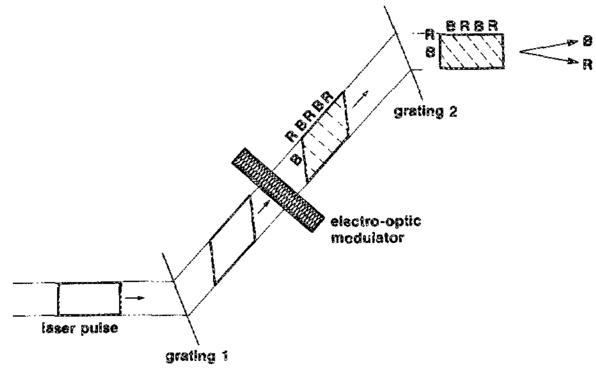

FIG. 3. The two-grating configuration. Grating 1 introduces a "predelay" that compensates for the time delay in beam amplitude produced by grating 2. By placing the first grating before the modulator, it is possible to correct the amplitude time delay without affecting the angular dispersion of the EO spectrum. The spectral angular distortion is optimized to produce high-efficiency frequency tripling. (The dashed lines are not wave fronts but contours of constant color.)

can be corrected by inserting an additional grating before the EO modulator (Fig. 3). (When the beam passes through the first grating, its residual bandwidth will, of course, be dispersed, but this dispersion is a negligible effect for a typical bandwidth-limited laser beam and will, in any case, be corrected by the second grating.) The main effect of the first grating is to introduce a time delay in the amplitude $E_0(t)$ opposite to the one that will be induced by the grating after the EO modulator. The time-delayed beam then passes through the modulator where the bandwidth is imposed. The grating after the EO modulator now serves a triple purpose (Fig. 3): (1) it restores the beam amplitude to its correct temporal shape; (2) it imposes the spatial frequency variation across the beam that is required for SSD; and (3) it imposes a spectral dispersion that can now be utilized for high-efficiency frequency tripling.

C. Frequency tripling

High-efficiency frequency tripling can be obtained by matching the spectral angular dispersion imposed by the grating to the angular dependence of the conversion crystals, so that each frequency component passes through the tripling crystals at its phase-matching angle (Fig. 4). This technique can only be applied for spectral dispersion in a single direction, along the angle-sensitive direction of the tripler. The conversion efficiency is a function of the beam angle and laser wavelength. For small deviations from opti-

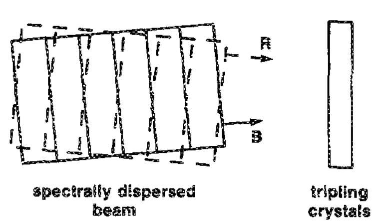

FIG. 4. High-efficiency frequency tripling of broad bandwidth light by spectral angular dispersion. (The separation of colors is grossly exaggerated in the figure. The angular spread is 200 μrad.)

mal conditions, the maximum conversion efficiency η_0 for a beam of constant intensity is degraded in the high-conversion regime ($\eta_0 \approx 0.9$), roughly according to [4,6]:

$$\eta = \eta_0[1 - (\delta\theta/\delta\theta_{90} + \delta\lambda/\delta\lambda_{90})^2], \tag{7}$$

where $\delta\theta$ is the deviation of the beam from phase-matching measured in air, and $\delta\lambda$ is the deviation of the fundamental wavelength. For the 1.6-cm crystals used on OMEGA, $\delta\theta_{90} = 100\,\mu$rad, $\delta\lambda_{90} = 0.6$ Å, and $\eta_0 = 0.9$ is attained at 1 GW/cm^2 (where the average over a temporal Gaussian is 0.75). In the small-signal regime, $\delta\theta_{90}$ and $\delta\lambda_{90}$ are a factor of 2 higher. In both regimes, the condition for optimal conversion is $\delta\theta/\delta\lambda \approx -165\ \mu$rad/Å. The maximum bandwidth consistent with high-efficiency tripling is determined by the maximum angular spread that can be tolerated for beam propagation and focusing on the target.

The current strategy for implementing SSD on OMEGA is to insert the diffraction gratings into the laser driver, thereby avoiding any additional optical elements at the end of the system. The spectral angular divergence imposed in the driver must then be able to propagate through the remainder of the laser chain and onto the target without significant energy loss or beam distortion. If we do not want the spread in the focused beam at the target plane to be larger than, say, half the target diameter D_T then

$$F\theta_{\mathrm{FW}} \lesssim \tfrac{1}{2} D_T,$$

where F is the focal length and θ_{FW} is the full-angle beam spectral divergence. For OMEGA, $F \approx 60$ cm and, for recent experiments, $D_T \approx 250\ \mu$m. Thus, the largest permitted divergence is $\sim 200\ \mu$rad, at the final focusing lens.

In order to remain within 10% of the maximum conversion efficiency with the permitted 200-μrad full-angle divergence, Eq. (7) shows that the bandwidth must not be greater than ~ 2 Å in the IR. This bandwidth would be too small to smooth the laser intensity on the time scale of interest (~ 50 ps) for the OMEGA experiments if the target were irradiated in the IR. However, upon frequency conversion, the frequency spread is tripled. Further, we can take advantage of "color cycling," as will be discussed below, to provide additional reduction in the smoothing time for the long-wavelength interference structure.

A second crucial issue, in addition to the tripling efficiency, is the question of how the frequency spectrum changes upon tripling; this will affect the averaging time and maximum uniformity achievable. We have calculated[7] the frequency tripling of the spectrally dispersed, phase-modulated beam in Eq. (5), using an extension of the analysis discussed in Ref. 8. The principal result is that for the modulated frequencies and bandwidths considered here, the frequency conversion can be treated in terms of the instantaneous frequency and propagation direction of the modulated light. Figure 5(a) shows the initial 2-Å bandwidth, and Fig. 5(b) shows the calculated tripled spectrum. The very slight asymmetry in the spectra is the result of coincidence between the high-frequency portion of the bandwidth and the peak of the pulse. A grating dispersion of 100 μrad/Å was used, producing a 5% reduction in the maximum conversion efficiency. The frequency spread has indeed tripled, and the electric field of the third harmonic is given by Eq. (5) with

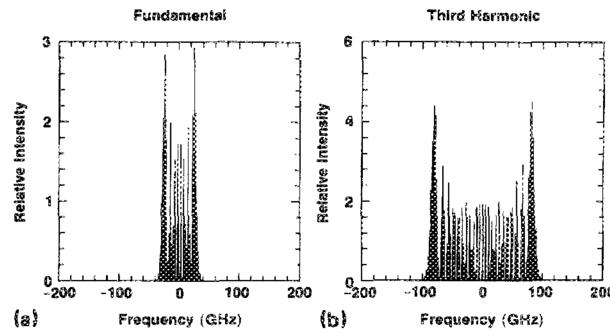

FIG. 5. Calculation of the intensity spectrum showing bandwidth tripling upon frequency tripling of a phase-modulated pulse. The modulation frequency is 2.5 GHz and the index is 12, corresponding to a frequency spread of 60 GHz. The slight broadening of each spectral line is due to the finite pulse width of 700 ps used in the calculation, and the slight asymmetry is due the modulation phase time relative to the peak of the pulse.

both ω and δ tripled, i.e.,

$$E_{3\omega}(Y,t) = E^0_{3\omega}(t)e^{i3\omega t + i3\delta\sin(\omega_m t + \alpha Y)}, \tag{8}$$

where $E^0_{3\omega}$ is a slowly varying function of time, corresponding to the Gaussian envelope of the input pulse. Physically, this is what would be expected, because the EO broadened light is oscillating from "red" to "blue" with only a small frequency range dominating at any instant of time. The entire small range is approximately phase matched to the crystal because of the angular dispersion of the grating. Under these conditions, the instantaneous frequency should triple, which is consistent with Eq. (8) and with initial experiments on SSD.[9,10] For the general case of broadband tripling, the tripling results would depend on the relative phases and amplitudes of the different spectral components.[7]

D. Diffraction grating considerations

We can now determine the grating configuration that would disperse the 2-Å bandwidth over 200 μrad at the output of the system. For the OMEGA laser, the gratings will be introduced at a stage in the driver where the beam is 2.9 times smaller than at the output. Since beam divergence is inversely proportional to beam diameter, the imposed dispersion must be 2.9 times larger, i.e., $\Delta\theta/\Delta\lambda = 2.9 \times (200\ \mu\mathrm{rad}/2\ \text{Å})$. The grating dispersion in the first order is given by[11]

$$\Delta\theta/\Delta\lambda = 1/(d\cos\theta), \tag{9a}$$

where d is the spacing between grooves on the grating and θ is the angle between the transmitted beam and the normal to the grating (Fig. 2). The incident and exit angles are related by the grating equation[11]

$$|\sin\theta_0 + \sin\theta| = \lambda/d. \tag{9b}$$

To keep the beam cross section circular, we require $\theta_0 = \theta$, yielding

$$\tan\theta = \tfrac{1}{2}\lambda(\Delta\theta/\Delta\lambda) \tag{10a}$$

and

$$d = [(\Delta\lambda/\Delta\theta)^2 + \tfrac{1}{4}\lambda^2]^{1/2}. \tag{10b}$$

Using the parameters for OMEGA, namely $\Delta\theta/\Delta\lambda = 290$

μrad/Å and $\lambda = 1.054\,\mu$m, we obtain the grating angle and line spacing: $\theta = 57°$ and $d = 0.63\,\mu$m. The maximum length L of the grating can be determined in terms of the beam diameter D_g at the grating (58 mm):

$$L = D_g / \cos\theta, \tag{11}$$

yielding $L = 10.6$ cm.

Note that the time delay t_D previously obtained in Eq. (6) can also be obtained from Fig. 2 using $t_D = L\,|\sin\theta + \sin\theta_0|/c$ together with Eqs. (9) and (11). For the above parameters, the time delay is 590 ps, approximately the pulse width in current OMEGA experiments, so that the pulse shape after the first grating in Fig. 3 is highly distorted.

E. "Color" cycling

The time delay across the grating can be used further to our advantage. Figure 3 shows that if the EO modulation time τ ($= 1/\nu_m$) is shorter than the time delay t_D (or $\alpha D > 2\pi$), then all the "colors" will cycle across the beam more than once at each instant in time. (The significant quantity is really a half-cycle, in which there is one complete sampling of the entire bandwidth). Thus, instead of the "red-blue" variation being distributed from one end of the DPP to the other, it can be distributed over smaller regions so that nearest elements will have a larger frequency difference, and their average interference pattern will smooth in a shorter time. For instance, with $\tau = t_D/3$, the smoothing time for nearest neighbors is three times shorter than if there had been only one color cycle. The price paid is that more distant DPP elements will have the same color, and their interference pattern will not smooth at all. However, the interference between distant elements produces shorter-wavelength structure that can be smoothed more easily within the target by thermal conduction of the deposited laser energy. The effect of color cycling is qualitatively similar to that produced by repeated echelon steps in the ISI technique.[3] However, as the number of cycles increases, the distance in Y between elements of similar color will decrease, and this interference will be more difficult to smooth. The optimal number of cycles will be discussed in Sec. IV.

To determine the relation between the number of color cycles N_c and the EO and grating parameters, we use the definition

$$N_c \equiv t_D\,\nu_m,$$

with t_D given by Eq. (6). Rewriting Eq. (6) in terms of the frequency spread ($\Delta\nu = \Delta\lambda c/\lambda^2$) and using $\Delta\nu = 2\delta\nu_m$, we obtain

$$N_c = D\theta_{\rm FW}/2\lambda\delta. \tag{12}$$

For the example of the 2-Å bandwidth ($\lambda = 1.054\,\mu$m) and $\nu_m = 2.5$ GHz, we have $\Delta\nu = 60$ GHz and $\delta = 12$. Using parameters evaluated at the final focusing lens ($D = 17$ cm and $\theta_{\rm FW} = 200\,\mu$rad) the number of color cycles is found to be $N_c = 1.4$. The entire bandwidth is displayed across the beam approximately three times.

Note that if the bandwidth is increased by increasing δ, then the number of color cycles is reduced, and we might not obtain as large of a reduction in the smoothing as would be expected. On the other hand, even if the bandwidth is kept constant, we might be able to reduce the smoothing time by increasing the modulation frequency (and simultaneously reducing δ), thereby increasing the color cycles.

III. SIMULATION RESULTS

To calculate the total electric field on the target (i.e., laser focal plane), we use scalar diffraction theory[12] to propagate the beam from the phase plate. The beam is first decomposed into its individual frequency components; each frequency is transported separately and then summed in the focal plane. The initial amplitude of each frequency component is determined by the frequency-tripling process, given by Eq. (8).

The scalar amplitude of this wave in the focal plane, after passing through the phase plate, is

$$U(x,y) = U_0\, e^{i3\omega t}\, \frac{\sin(n\gamma + q)}{n\gamma + q}\, \frac{\sin p}{p} \times \sum_{KL}\sum_n J_n(3\delta)\, e^{i(n\omega_m t - 2n\gamma L - 2Lq - 2Kp + \phi_{KL})}, \tag{13}$$

where KL corresponds to a DPP element, and ϕ_{KL} is the phase imposed by that element. The variables (p,q) are related to the coordinates (x,y) in the focal plane by $(p,q) = (x,y)k\Delta/2F$, where k is the wave number of the frequency-tripled fundamental, Δ the distance between phase-plate elements, and F the focal length (Fig. 1). The variable t is the modified time parameter $t - Z/c$ from Eq. (5), and $\gamma = \alpha\Delta/2$.

One effect of the spectral angular dispersion is to shift the center of the diffraction envelope for each mode in the $q(y)$ direction. The envelope is no longer the same in the x and y directions; this can introduce long-wavelength modes of irradiation nonuniformity. For the small bandwidth used here, the distortion is relatively small and can be compensated for by using rectangular DPP elements so that the ratio of the y to x lengths is ~ 1.6 (Fig. 6). This reduces the diffraction size of the beam in the y direction to approximately compensate for the spread caused by the spectral dispersion. The effect on Eq. (13) is to multiply q by 1.6.

The time-averaged, single-beam intensity in the focal plane is

$$I(x,y) = \frac{1}{\Delta t}\int_0^{\Delta t} |U|^2\, dt. \tag{14}$$

It is instructive to examine the asymptotic limit of the intensity when averaged over large times. Using Eq. (13), we have

$$I(\Delta t \to \infty) = U_0^2 \sum_n J_n^2(3\delta)\, \frac{\sin^2(q + n\gamma)}{(q + n\gamma)^2}\, \frac{\sin^2 p}{p^2} \times \sum_{\substack{K,L\\K',L'}} \cos\,[2(n\gamma + q)(L - L') + 2p(K - K') + \phi_{KL} - \phi_{K'L'}]. \tag{15}$$

Each color produces the same interference pattern, but shifted in the y direction and with a relative amplitude J_n^2. The different patterns add up incoherently as would occur if we had attempted to smooth the irradiation nonuniformities by an oscillatory shift of the beam. However, at intermediate

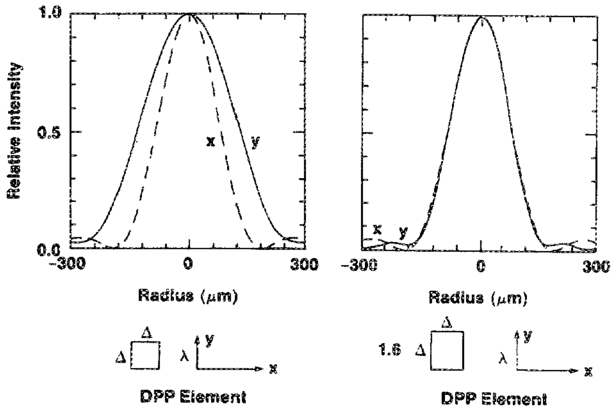

FIG. 6. Correction of the beam ellipticity in the target plane by elongating the phase-plate elements in the direction of frequency dispersion. This reduces the diffraction spread in that direction, in part compensating for the angular spectral dispersion.

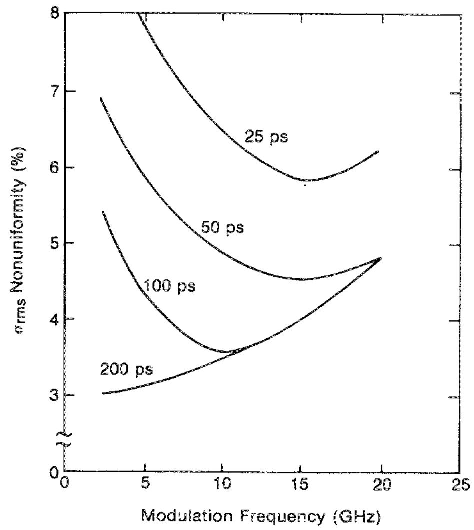

FIG. 7. The effect of EO modulation frequency on the rms nonuniformity for 24-beam irradiation. Smoothing over 1% of the target radius was used. In all cases, the IR bandwidth is 2 Å. For smoothing times below 100 ps, frequencies of 10–15 GHz are optimal, corresponding to 6–9 color cycles across the beam.

times there is a difference between SSD and simple beam deflection. With beam deflection, a large part of the target will not be irradiated at times of maximum deflection, producing the effect of beam mispointing. With SSD, the target is always completely irradiated. A relatively smooth overall beam profile is obtained, even if the intensity is averaged in only one direction, because the speckle interference pattern varies rapidly and somewhat randomly across the beam. Since the "color" deflection is up to one-half the target radius, even long wavelength nonuniformities are reduced.

The intensity as a function of averaging time [Eq. (14)] was evaluated numerically for several values of the modulation frequency and bandwidth. The calculations were performed using a 75×75 phase plate with the rectangular elements of Fig. 6. (OMEGA currently uses 125×125 square phase-plate elements.) The effect of a larger number of elements (with a smaller f number to keep a constant focal spot size) is to move the irradiation nonuniformity to shorter wavelengths[3] which would be smoothed more effectively. The intensity in the focal plane was evaluated with the resolution of a 200×200 grid extending to the first zero of the diffraction envelope. The target radius was chosen equal to the radius of the 10% intensity contour of the beam which enclosed about 80% of the beam energy (typical of OMEGA experiments). The calculated focal plane image was averaged over a square region of ±1 grid element, corresponding to a smoothing of $\sim1\%$ of the beam radius, and the profile was then repeatedly mapped onto the surface of the target to determine the uniformity of irradiation from multiple overlapping beams. This mapping would be most appropriate early in the laser pulse before a substantial plasma atmosphere has been created and before refraction becomes important. At this time, irradiation uniformity must be the highest because a large separation distance between the critical and ablation surfaces has not been established, and thermal smoothing of nonuniformities in energy deposition will be minimal. Typical hydrodynamic implosion simulations show that near the peak of the pulse, the smoothing distance can be many times larger than the amount used here.

The reduced smoothing time produced by "color cycling" is demonstrated in Fig. 7. Plotted is the rms nonuniformity (using the OMEGA 24-beam geometry) as a function of modulation frequency for different averaging times. As the modulation frequency changes, the modulation index is adjusted to keep the IR bandwidth at 2 Å. The modulation frequency determines the number of color cycles according to: $N_c = t_D\,\nu_m$. For $t_D = 590$ ps (Sec. III E), we have $N_c = 0.6\,\nu_{\rm GHz}$. The optimal modulation frequency for these conditions is found to be ~10 GHz ($N_c = 6$), for $\Delta t < 100$ ps. The level of $\sigma_{\rm rms} = 5\%$ is reached after a 50-ps smoothing time at 10 GHz, which is less than half the time that is required at 2.5 GHz. However, for averaging times greater than ~150 ps, the 2.5-GHz curve asymptotes to a value 15% lower than the 10-GHz case. (Initial SSD experiments on the OMEGA laser system used 2.5 GHz, because this was the easiest to implement at the time.)[9] For frequencies greater than ~15 GHz, the asymptotic nonuniformity is degraded by too many repetitions of the same color.

The residual asymptotic nonuniformity has three sources: First, bandwidth is dispersed only in the y direction so that all phase elements in the x direction have the same frequency (for a given y); these will form a time-independent interference structure. Second, the different frequencies are weighted very differently (Fig. 5); a uniformly distributed spectrum would reduce the nonuniformity by $\sim50\%$. Third, the interference structure repeats itself after a modulation time.

Although Fig. 7 was calculated for a 2-Å bandwidth, the results can be scaled to any other bandwidth with the same total angular divergence (i.e., the grating dispersion $\Delta\theta/\Delta\lambda$ is changed inversely with the bandwidth to maintain a 200-μrad divergence at the focusing lens). The scaling is evident from the form of the electric field E_D in Eq. (5), which depends only on the product $\omega_m t$ and on δ. (Note that α depends only on δ for a given $\Delta\theta$.) Thus, doubling the band-

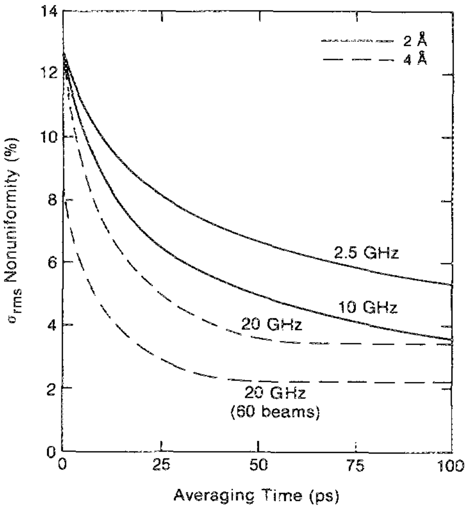

FIG. 8. The reduction in rms irradiation nonuniformity as a function of averaging time. Compared are the effects of (1) increasing the modulation frequency from 2.5 to 10 GHz for a 2-Å bandwidth, (2) increasing the bandwidth to 4 Å and doubling the modulation frequency, and (3) increasing the number of beams from 24 to 60.

width by increasing ω_m and keeping δ constant will produce the same smoothing on E_D, but in half the time.

The effects of increasing the modulation frequency, increasing the bandwidth, and increasing the number of beams, are shown in Fig. 8, where σ_{rms} is now plotted as a function of time. Shown is the improvement possible with color cycling by increasing the modulation frequency from 2.5 to 10 GHz at a 2-Å bandwidth. Increasing the bandwidth to 4 Å together with doubling the modulation frequency cuts the smoothing time in half with the nonuniformity asymptoting to $\sigma_{rms} = 3.5\%$ at 50 ps. These calculations were performed for 24 beams. One way to reduce the asymptotic nonuniformity is to increase the number of beams. The results for 60 uniformly disposed beams show almost a factor of two reduction in nonuniformity.

The predicted factor of ~ 3 reduction in σ_{rms} for 24 beams using SSD could significantly improve results for current OMEGA high-density experiments, and this improvement can be attained with relatively straightforward modifications in the laser system.

IV. SUMMARY

A relatively simple form of SSD has been investigated. It is simple in the sense that all new optical elements are installed in the driver, and no additional components are required at the end of the system. An EO frequency-modulated pulse is used for the bandwidth to prevent the formation of high-intensity spikes that could damage the laser glass, as might occur with a "chaotic" form of bandwidth. The essential spatial variation of colors on the DPP and the angular dispersion for frequency tripling are accomplished with a set of diffraction gratings that take advantage not only of the dispersion properties of the gratings but also their time-delay characteristics.

The same features that make this technique relatively simple also limit the maximum bandwidth to ~ 2 Å for OMEGA. The primary limitation is the divergence that can be tolerated at the focusing lens, which sets the maximum bandwidth that can be fully compensated for frequency conversion. Larger bandwidths can be employed, but a tradeoff is then required between reduced conversion efficiency and improved uniformity on target. For example, the bandwidth on OMEGA could be increased to 4 Å, while maintaining a 200-μrad divergence, at the expense of about a 15% reduction in conversion efficiency. SSD would obviously benefit from the development of large-aperture crystals of material less sensitive to bandwidth than KDP. However, even with 2 Å, rapid smoothing times can be achieved, because the frequency spread is tripled upon frequency conversion and because we can employ "color cycling." Computer simulations show that this version of SSD can reduce the rms nonuniformity on OMEGA by factors 2–3 in averaging times of 25–50 ps.

Further improvements in uniformity are possible with SSD, by employing additional techniques to reduce the interference structure. These are presently under investigation.

ACKNOWLEDGMENTS

This work was supported by the U. S. Department of Energy Office of Inertial Fusion under Agreement No. DE-FC03-85DP40200 and by the Laser Fusion Feasibility Project at the Laboratory for Laser Energies which has the following sponsors: Empire State Electric Energy Research Corporation, New York State Energy Research and Development Authority, Ontario Hydro, and the University of Rochester. Such support does not imply endorsement of the content by any of the above parties.

[1] T. Kessler *et al.*, LLE Rev. **33**, 1 (1987).
[2] Y. Kato, K. Mima, N. Miyanaga, S. Arinaga, Y. Kitagawa, M. Naktsuka, and C. Yamanka, Phys. Rev. Lett. **53**, 1057 (1984).
[3] R. H. Lehmberg, A. J. Schmitt, and S. E. Bodner, J. Appl. Phys. **62**, 2680 (1987).
[4] R. S. Craxton, S. Skupsky, and J. M. Soures, LLE Rev. **36**, 158 (1988).
[5] A. Yariv, *Quantum Electronics*, 2nd ed. (Wiley, New York, 1975), Sec. 14.4.
[6] R. S. Craxton, S. D. Jacobs, J. E. Rizzo, and R. Boni, IEEE J. Quantum Electron. **QE-17**, 1782 (1981).
[7] R. W. Short and S. Skupsky (unpublished).
[8] R. C. Eckardt and J. Reintjes, IEEE J. Quantum Electron. **QE-20**, 1178 (1984).
[9] T. Kessler *et al.*, LLE Rev. 37, 40 (1989).
[10] M. D. Skeldon, T. Kessler, R. S. Craxton, S. Skupsky, W. Seka, R. W. Short, and J. M. Soures (unpublished).
[11] M. Born and E. Wolf, *Principles of Optics*, 6th ed. (Pergamon, New York, 1980), pp. 403–406.
[12] *Ibid.*, pp. 436–437.